

Instrumentation for Testing Soft-Tissue Undergoing Large Deformation: *ex vivo* and *in vivo* studies

Tie Hu^a, Alan C. W. Lau^b, and Jaydev P. Desai^{*c}

*Robotics, Automation, Manipulation, and Sensing (RAMS) Laboratory

University of Maryland, College Park, MD, USA

Abstract – Biomechanical property of soft tissue derived from experimental measurements is critical to develop a reality-based soft-tissue model for minimally invasive surgical training and simulation. In our research, we have focused on developing a biomechanical model of the liver with the ultimate goal of using this model for local tool-tissue interaction tasks and providing feedback to the surgeon through a haptic (sense of touch) display. In this paper, we present two devices that we have designed and built, namely *ex vivo* and *in vivo* testing devices. We used them to measure the experimental force and displacement data of pig liver tissue. The device for *ex vivo* experiments uses a PC-based control system to control the motion of the probe and acquire the experimental force and displacement data. The force resolution for *ex vivo* testing was 0.002 Newton (as per the resolution information provided by the manufacturer) and the probe velocity ranged from 0.1 mm/sec to 25.4 mm/sec. The device was designed so that it could be easily used for both small probe (tissue sample larger than the indenting probe surface area) testing as well as large probe (tissue sample smaller than the indenting probe surface area) testing. The device for *in vivo* experiments used a microcontroller-based instrumentation to control the motion and acquire and store the data on a multimedia memory disk. This device is designed for the purpose of acquiring experimental force and displacement data *in vivo*. The primary challenge in the design of the device for *in vivo* experiments was the limited workspace for device operation. The force

^aDr. Tie Hu is with the Department of Computer Science at Columbia University, NY 10027 USA.

^bDr. Alan C.W Lau is with the Department of Mechanical Engineering and Mechanics at Drexel University, Philadelphia, PA 19104, USA (e-mail: lau@drexel.edu)

^cCorresponding author. Dr. Jaydev P. Desai is the Director of Robotics, Automation, Manipulation, and Sensing (RAMS) Laboratory in the Department of Mechanical Engineering at University of Maryland, College Park, MD 20742, USA. (e-mail:jaydev@umd.edu).

This work was supported in part by NSF grant EIA-0711040.

Portions reprinted, with permission, from:

1. Tie Hu; Desai, J.P.; Castellanos, A.E.; Lau, A.C.W., "Modeling In vivo Soft Tissue Probing", The First IEEE/RAS-EMBS International Conference on Biomedical Robotics and Biomechanics, 2006, BioRob 2006, February 20-22, 2006 Page(s):537 – 542. © [2006] IEEE.
2. Tie Hu; Desai, J.P.; Lau, A.C.W., "Direct and inverse problem models for large soft-tissue deformation: Application to haptic feedback in surgical simulation", Proceedings of 12th International Conference on Advanced Robotics, 2005, ICAR '05, 18-20 July 2005 Page(s):445 – 451. © [2005] IEEE.
3. Hu, T.; Desai, J.P., "Soft-tissue material properties under large deformation: strain rate effect", 26th Annual International Conference of the IEEE Engineering in Medicine and Biology Society, 2004, IEMBS '04, Volume 1, 2004 Page(s):2758 - 2761 Vol.4. © [2004] IEEE.

resolution for *in vivo* testing was 0.015 Newton and the displacement resolution was 0.02 mm. The sampling frequency for data acquisition for *in vivo* testing was 50Hz.

***Index Terms* – *ex vivo* and *in vivo* soft-tissue modeling; surgical simulation; Local effective elastic modulus (LEEM).**

I. INTRODUCTION

Reality-based modeling of soft tissues is critical for providing accurate haptic feedback to surgeons in surgical training and simulation. By reality-based modeling, we are interested in modeling tissues as accurately as possible by determining the mechanical properties from actual experiments. In the literature, most modeling efforts assume the mechanical properties of the soft tissue and propose methods to efficiently solve the tissue simulation problem for robot-assisted surgery/training.

“Global” elastic deformations of real and phantom tissues have been studied extensively in previous work, through simple poking interactions [1]. An alternate approach to validate models with pre-located inclusions has been studied as well [2, 3]. There has also been research on estimating the mechanical properties of the tissue through high-frequency shear deformations of the tissue sample, and elastography techniques. A variety of other techniques also exist in the literature for estimating the viscoelastic characterization of tissues, for example, [4, 5]. Ottensmeyer [6] and others have performed tissue experiments to characterize force vs. displacement for pig liver tissue. The quantitative knowledge of the biomechanical property of tissue is essential for soft tissue modeling. Fung [7] showed that the elasticity property of rabbits’ mesentery could be simply expressed as an exponential function. Tong [8] derived the constitutive equation describing the stress and strain relationship of the skin. It has been known that soft tissue has extremely nonlinear stress-strain relationship, which makes it difficult to model large strain deformations. To develop a liver model for probing, it is necessary to characterize the material properties of the liver over a large range of deformation consistent with the range of deformation in surgery. Hence, it is necessary to derive the biomechanical properties of the liver, which is valid for both small and large strain regions [9]. The theory of elastic material subjected to large deformations has been used to model the physical behavior of the biological tissues [10]. Farshad [11] studied the material characterization of the pig kidney and used the Blatz model to model the uniaxial compression test. Davies [12] developed a mathematical model for spleen tissue, which is applicable to keyhole surgery. Miller [13] developed a constitutive model of the livers of Rhesus monkey based on the experimental results of Melvin [14]. In their studies, the tissues were assumed as incompressible (no volume change during deformation), homogeneous (same tissue composition throughout), and isotropic (no directional preference) elastic material.

In recent years, a number of groups have developed the instrumentation for *in vivo* abdominal organs. Ottensmeyer [6] developed a minimally invasive instrument which can perform the normal indentation on solid organs, apply and measure the deformations over a frequency range from DC to approximately 100Hz. Nava [15] used an aspiration device to measure the mechanical properties of human liver and kidney. Carter [16] used a sterile hand-held compliance probe to obtain the data from live patients. To measure the tissue properties accurately, it is important to build devices that can measure the tissue response to probing for both *ex vivo* and *in vivo* tests. Consequently, this paper presents two devices that we have designed and built for the purpose of *ex vivo* and *in vivo* soft-tissue testing.

In vivo experiments are affected by the temperature, the protein break-down within the tissue during testing, incompressibility, and blood perfusion. The mechanical properties of *in vivo* soft tissues are critical to develop a reality-based surgical simulator. However, it is a challenging task to perform *in vivo* testing since the *in vivo* testing device has to operate in a limited workspace. Since the traditional tests for *ex vivo* (lateral shear and normal bi-axial stress) can not be applied to *in vivo* testing, most *in vivo* testing is done through localized indentation or aspiration of tissue [15].

We were motivated to develop a portable *in vivo* testing device, which is compact and has an integrated mechanical and electronic system. The device has the capability to be attached to a surgical retractor and perform motion control, data acquisition, and data storing. There is no additional need of data acquisition board, motion control card, and PC. We chose the microcontroller as the core device to control the stepper motor, acquiring the force and displacement data from load cell and linear displacement sensor, and store the data in a USB flash disk. The post data processing can be done in the laboratory PC. This device can also be used to measure the real-time force and displacement data of electrocautery tool and surgical scalpel.

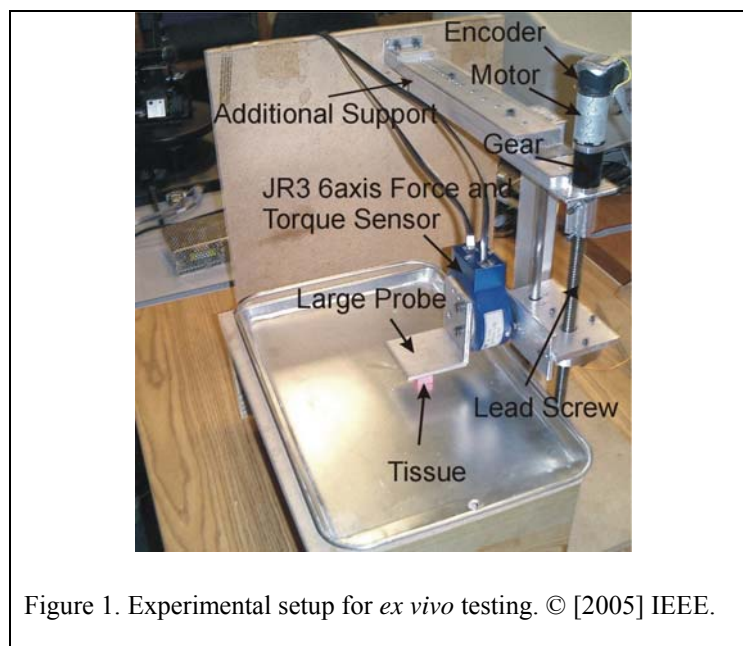
The rest of this paper is organized as follows. In section II, we present the design and development of *ex vivo* and *in vivo* soft-tissue testing devices. We also present the experimental setup for *in vivo* experiment. In section III, we present the experimental results from *ex vivo* and *in vivo* tests. Finally in section IV, we make some concluding remarks.

II. MATERIALS AND METHODS

2.1 *Ex vivo* Tissue Testing Device

We have designed and developed a tissue compression apparatus, which can measure the compressive force and displacement. Figure 1 shows the configuration of our test device for *ex vivo* tests. The system consists of a motion control part, a force measuring part, and a post-data processing part. The motion control part is a lead screw assembled with a geared DC motor and encoder (Maxonmotor, Inc., Fall River, MA, USA), which is supported by two horizontal supports. The

anti-backlash nut in the lead screw prevents any backlash in the mechanism. A JR3 6-axis force/torque sensor (manufactured by JR3 Inc., Woodland, CA, USA; model 20E12A-I25, with resolution of $2e-3$ N in F_x , F_y , and F_z , and 2.5×10^{-5} Nm in T_x , T_y , and T_z) is attached to the probe as shown in Figure 1. Since this force sensor does not have in-built filter in its hardware to filter the data, we filtered the experimental data off-line. When the motor rotates, the probe moves as per the motion control command. The position of the probe is controlled by the dSPACE DS1103 controller board (dSPACE, Inc.) and it also records the force and displacement data. The sampling frequency for control and data acquisition is 1000 Hz. The algorithm implemented in the dSPACE card is a proportional +derivative (PD) control scheme. The communication between the dSPACE card and the JR3 data acquisition card is accomplished by CLIB library (dSPACE, Inc.). The size of the probe is 50 mm x 50 mm and the surface is polished and covered with petroleum jelly to minimize the contact friction force. The size of the probe ensures that the liver sample fully contacts with the probe surface and contact over the entire surface is maintained during compression. Secondly, the larger size of the probe was used to obtain the bulk response of the soft-tissue during compression tests. We assume that over the entire range of compression the volume of the sample is conserved (though in reality this is not generally true).



For *ex vivo* testing, liver samples were taken from freshly slaughtered pigs and transported to the laboratory within 2 hours post mortem. We used a tube (25.4mm outer diameter and 22.2mm inner diameter) with a sharp edge at the perimeter to prepare cylindrical samples for our experimental trials. A group of samples were cut from the same lobe of the liver since our experimental results indicated that the property variation across lobes could be sometimes significant. In the compression experiment, the liver sample was compressed up to 30% strain of its nominal thickness. In the quasi-static analysis, the probing speed was 0.1 mm/sec, while at higher strain rates the probing speeds used were 5.08 mm/sec, 12.7 mm/sec and 25.4 mm/sec.

2.2 *In vivo* Tissue Testing Device

Due to workspace constraints during *in vivo* testing, we were motivated to develop a portable *in vivo* test device, which has compact size and an integrated mechanical and electronic system. Figure 2 shows the CAD model of the device. It was necessary that this device be attached to the surgical retractor and performs motion control, data acquisition and data storing in one device. In our current design, there is no additional need of data acquisition board, motion control card, and PC. We chose the microcontroller as the core device to control the stepper motor, acquiring the force and displacement data from load cell and linear displacement sensor, and then store the data in a USB flash disk. The post data processing can be done in the lab PC. This device can also be used to measure the real-time force and displacement data of electrocautery tool and surgical scalpel.

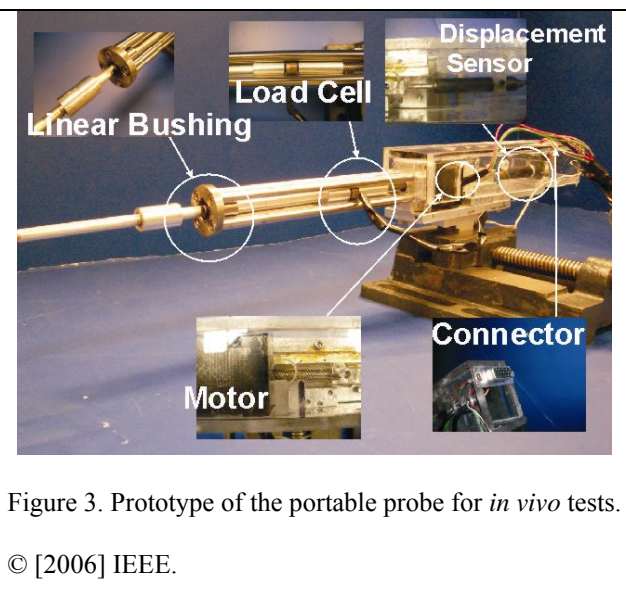
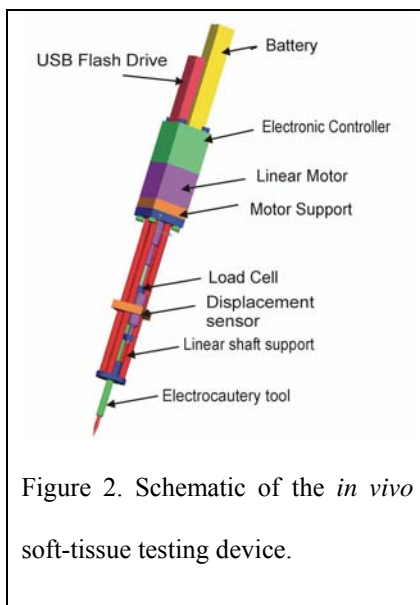
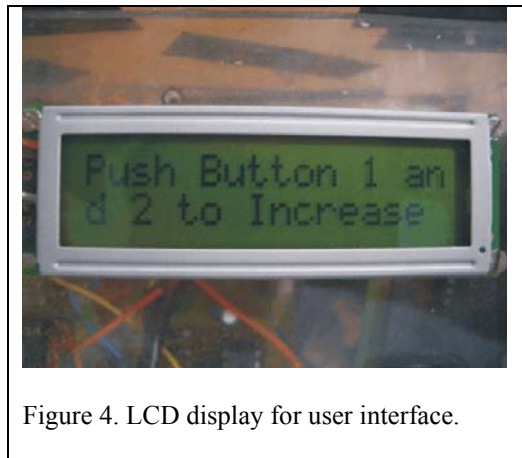
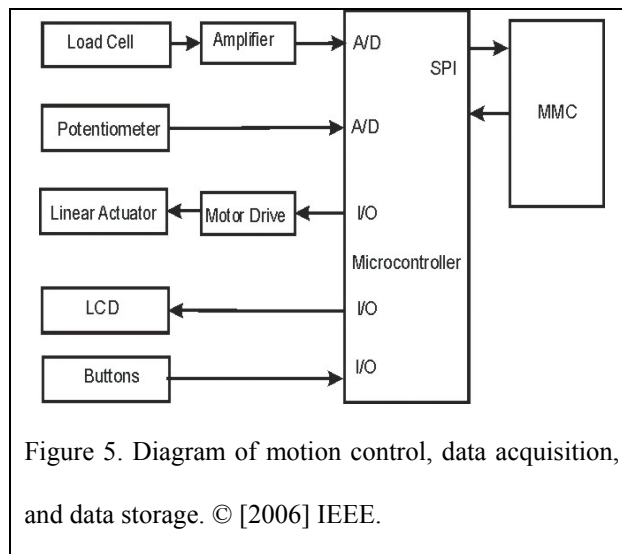


Figure 3 shows the prototype of portable probing device that we developed for *in vivo* experimental measurements. In this prototype, we modified our initial design by separating the motion and sensing mechanism from the electrical controller and data acquisition. The mechanism and controller are connected by power wires, signal and control wires. The device consists of a linear stepper motor (Haydon Swith & Instrument, Model 35000, Size 14, 20 Newton thrust force at 400 steps/sec), a sensotec subminiature load-cell (Model 11, 44.5 Newton load range, infinite resolution, foil strain gage type), and a linear displacement sensor (Omega, Model LP804, 25mm stroke range, incremental sensitivity 0.001 mm). A linear bushing with a flat flange (MISUMI, LHFR 6) is connected with the motor supporter via the four 150mm-length shafts. The bushing guides the probe and reduces the friction force. The load-cell is mounted between the probe head and the motor shaft. A linear displacement sensor is attached to the other end of the shaft. The motor shaft is also attached to a linear guider to prevent the rotational motion. When the shaft is driven by the motor, the force applied on the head of the probe is transmitted to the load-cell. All control and

signal wires in the probing mechanism are connected to a 25-pin D-SUB connector. A cable with D-SUB connector is used to connect the controller and the mechanism. The probe can be attached with a surgical retractor by a fixture under the mechanism. To prevent the rupture of the liver capsule, the probe head was machined into a hemi-spherical shape with a diameter of 7 mm.

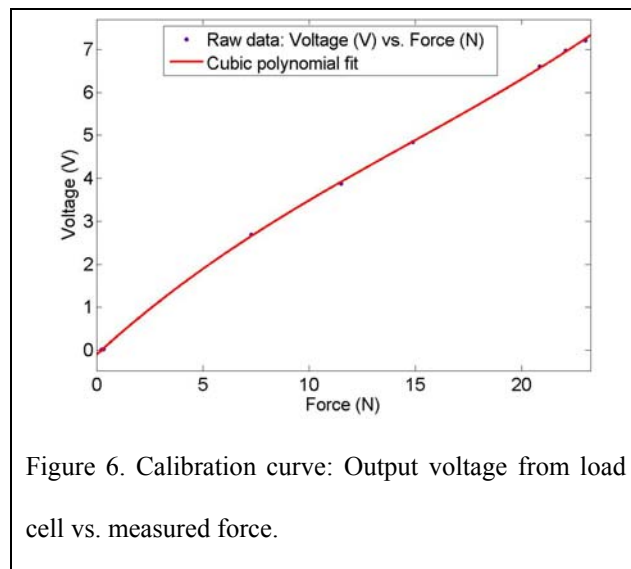


The function of controller is to control the motor velocity and displacement, acquire the force and displacement data, store the experimental data on a storage device, and provide a user interface (see Figure 4) to the operator. The controller controls the motion of the probe and acquires the experimental data, which is connected with the probing mechanism by the cable. We use an 8-bit AVR microcontroller ATMEG16 (ATMEL). It controls the stepper motor controller circuit, acquires the signal from the strain-gage amplifier and linear displacement sensor, and stores data in a SANDISK 128 MB Multimedia Memory Card (MMC). ATMEG16 microcontroller is a powerful RISC microcontroller with 32 general I/O ports, 8 channels of 10-bit ADC and a Serial Peripheral Interface (SPI). The 10-bit ADC can achieve force resolution of 0.015 Newton and displacement resolution of 0.02 mm. SPI is a common interface between the microcontroller and the other peripheral devices. In the system, it was used to communicate the microcontroller with MMC. We designed a standard three-op-amp instrumentation amplifier circuit (Linear Technology, LT1169 Op Amp) to amplify the signals from the load-cell. A step-motor driver (ST Microelectronics, L297 step-motor controller, L298 dual bridge driver) was made to drive the linear actuator. The operational frequency of the circuit was 4 MHz. A timer interrupt was implemented to realize the real-time data acquisition and motor control. The sampling time for data acquisition was 50 Hz. We use LCD and push button as user interface to start and stop the motor motion. Figure 4 shows the LCD display we used for our device and Figure 5 shows the overall controller schematic.



In the device, we used the multimedia memory card as data storage device. MMC is an ideal storage device for a small data acquisition device used in laboratory. The experimental data is recorded as FAT16 (File Allocation Table) format in MMC. It enables the data file to be opened as the text file in windows operating system for post-processing. The firmware of the controller was developed by CodeVision AVR C Compiler (Hp Info Tech). We developed a library to write the experimental data into MMC as FAT format.

2.3 Calibration of In vivo Probe



The probe was calibrated by a JR3 6 axis force/torque sensor (model, 851435A-140) and a Tektronix multimeter (TX3 True RMS). The multimeter measured the voltage from the instrumentation amplifier of the load-cell.

Figure 6 shows the relationship between the output voltage and the measured force from the load cell. It is expressed as:

$$V = 0.00028F^3 - 0.012F^2 + 0.4516F - 0.09913 \quad (1)$$

Where V is the output voltage from the load cell in volts and F is the measured force in Newtons. The R^2 value of the fit was 0.9999.

We use a dial caliper (0.001” resolution) as the calibration tool to measure the displacement of linear displacement sensor. We got the following relationship between the actual displacement and the voltage output from linear displacement sensor when the applied voltage is 5.07 volts.

$$\text{Displacement(mm)} = (0.194 \times \text{voltage(Volts)} + 1.538) \times 25.4 \tag{2}$$

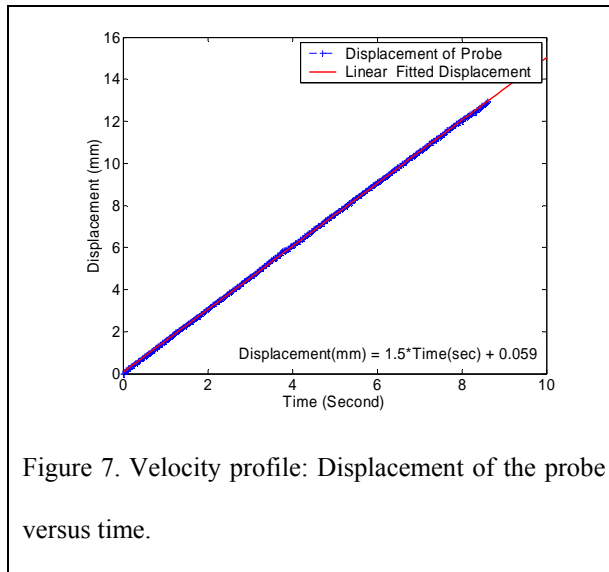


Figure 7. Velocity profile: Displacement of the probe versus time.

Figure 7 shows plot of displacement versus time. The motor speed (in this case the slope of the line, 1.5mm/sec) can be changed by adjusting the pulse frequency sent to motor drive.

2.4 *In vivo* Soft-tissue Measurements - Experimental setup

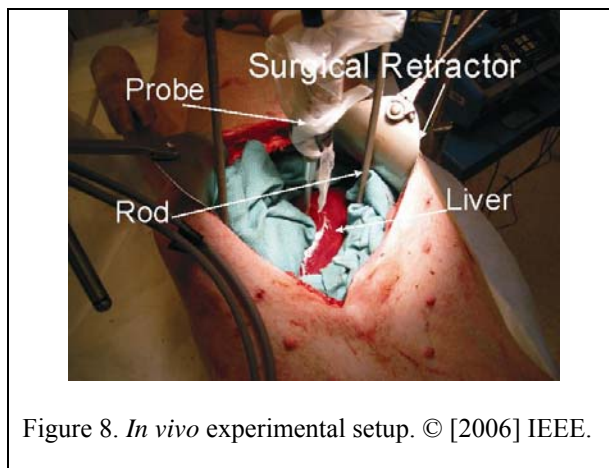


Figure 8 shows the experimental setup for *in vivo* soft tissue testing. The abdomen of a pig (50 pounds) under general anesthesia was opened by a surgical electrocautery tool and retracted by a surgical retractor (Thompson, Inc.). A clamp was made to attach the probe the tractor. The height of the probe can be adjusted by raising or lowering the stainless steel assembly. Due to the unconstrained boundary conditions of liver, it is necessary to create some constraints for the test. A stainless plate of size 100mm X 100mm was

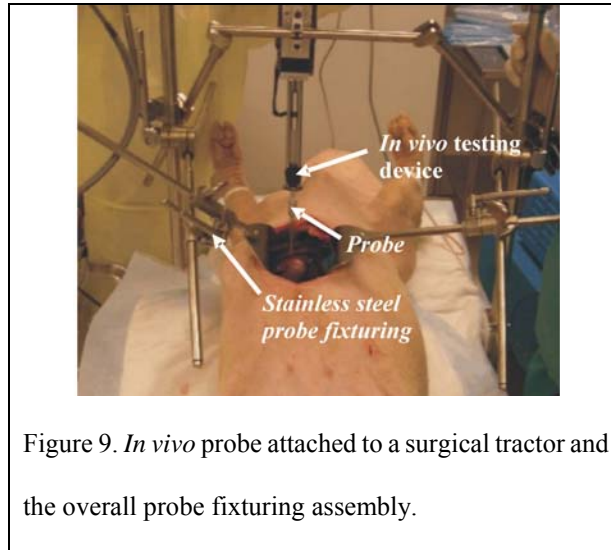
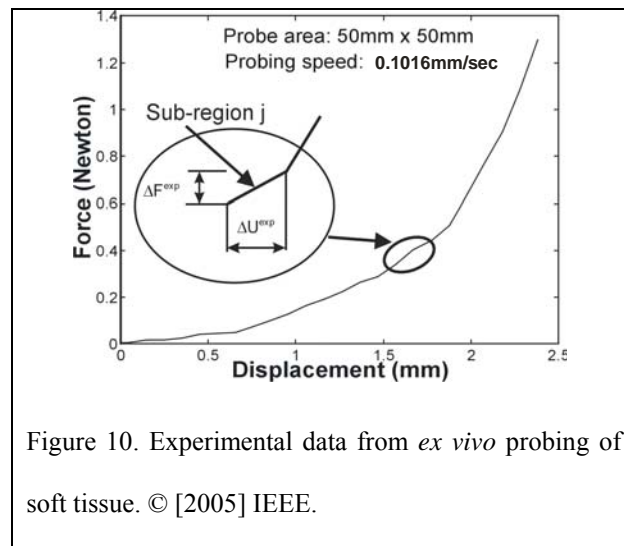


Figure 9. *In vivo* probe attached to a surgical tractor and the overall probe fixturing assembly.

inserted under the liver. Two rods, one on each end of the plate was used to support the plate. The rods were attached on the other end to the stainless steel fixturing assembly as shown in Figure 9. To prevent the movement of the liver, the surroundings of the liver were stuffed with the surgical sponge. The probe was attached to the support of the retractor and positioned approximately to enable probing on the liver surface. The thickness of liver in the position of probing was about 30 mm. The liver was poked at speed of 1.5mm/sec to replicate quasi-static measurements. A respirator machine helped the pig to breathe during the experiments. However, the regular movement of liver caused by the respirator had obvious influence on the results of the test.

III. RESULTS

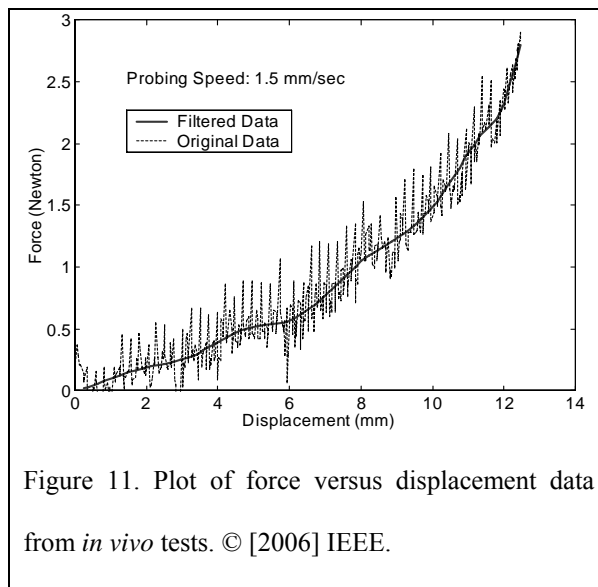
3.1 *Ex vivo* Test



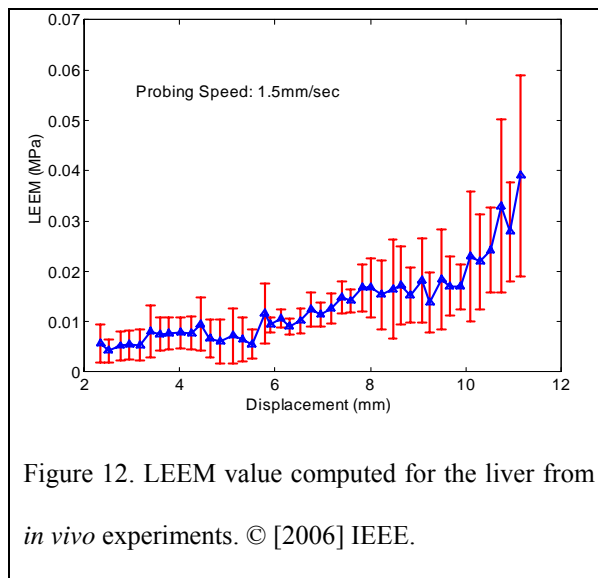
In surgery, surgeons probe the liver tissue with variable speed over a large range. The force vs. displacement data of the tissue is monotonic and nonlinear (Figure 10). The data were filtered with a low-pass filter after it was captured from the force sensor. The nonlinear curve can be considered as formed by linking many sub-regions (or sub-segments). Inside each sub-region, the variation of the force increment ΔF with the displacement increment ΔU is idealized to be linear (see insert of Figure 10). Hence in our models, the globally nonlinear force-displacement curve is closely approximated by a piecewise-linearization curve. This is used to compute the local effective elastic modulus (LEEM) of the tissue during tissue compression tests. In the large probe experiments, we assumed that the tissue undergoes uniform deformation and there is zero lateral stress on the top and bottom surfaces, and the sides of the sample. The displacement of the top surface of the tissue is the same as the displacement of the probe. The tissue is assumed as the incompressible material so the volume of the tissue is conserved.

3.2 *In vivo* Test

In vivo experiments were performed to measure the force and displacement data of tissue undergoing large deformation. Figure 11 shows the force versus displacement data for a sample *in vivo* measurement. The raw data was filtered by a 5th order Butterworth filter at 1.375 Hz, since the raw data was noisy.



The tissue was indented at a speed of 1.5 mm/sec to simulate quasi-static analysis. We computed the LEEM values for similar displacement of the soft tissue across all trials. Figure 12 shows the plot of the ABAQUS-computed LEEM for five trials [17]. From this figure, we observed some characteristics of LEEM. Physically, LEEM is the local slope of the stress-strain curve. It signifies the local deformation resistance of the material with each infinitesimal increase of displacement. We can separate the LEEM versus displacement plot into two characteristic regions. In the initial smaller deformation region (approximately 0 to 15% compression), the LEEM is small and increases slowly. In the larger deformation region (approximately 15 to 40% compression), the LEEM increases non-linearly and rapidly. Considering the rotational symmetry in the specimen geometry, material and loading, an axisymmetric FE model was constructed with bilinear 4-node axisymmetric elements (element type CAX4 in ABAQUS). The size of model is 50mm X 30mm. The bottom of the model is constrained vertically so that it cannot move in the vertical direction. The central line is constrained so that the elements on the central line can move vertically. The right edge of the model is also constrained to prevent the movement of elements horizontally, however, the elements can move vertically. To achieve a reasonable computation time and suitable precision in the results, the meshes were divided into two parts, namely fine and coarse mesh. The fine mesh has a size of 25mm X 30mm and a total of 1980 elements. The coarse mesh has a size of 25mm X 30mm and 150 elements. Comparing the *in vivo* tests with *ex vivo* tests for quasi-static analysis, we conclude that the LEEM values in *in vivo* measurements are significantly lower compared to *ex vivo* measurements. This could be due to the absence of incompressibility in *in vivo* measurements as well as perfusion. Our subsequent work will focus on high strain rate measurements during *in vivo* soft-tissue testing and we will compare the data with our prior work on *ex vivo* soft-tissue testing [17, 18, 19, 20]. Details of the modeling approach are presented in [21].



IV. CONCLUSIONS

In this paper, we presented two devices, one for *ex vivo* and the other for *in vivo* soft-tissue measurements. We have designed and developed a tissue compression apparatus for characterizing the mechanical response of *ex vivo* liver tissue for compression experiments using a large probe. We measured the force versus displacement data at quasi-static and higher strain rates for probing experiments. Like most soft tissue, liver tissue has an extremely nonlinear stress versus strain relationship during probing. It is thus critical to characterize the material properties of the liver over a large range of deformation consistent with the range of deformation in surgery. In our initial work, the liver tissue was assumed to be incompressible, isotropic, and homogeneous material. Based on the experimental data, we were able to develop a large probe model for the liver tissue. The tissue was compressed up to 30% strain of its nominal height.

We also designed and developed an apparatus for characterizing the mechanical response *in vivo* of liver tissue using a small probe. The device has the capability to acquire in real time the force and displacement data. The experiment was performed on the liver of a pig under general anesthesia. Like most soft tissue, liver tissue has an extremely nonlinear stress versus strain relationship during probing. It is thus critical to characterize the material properties of the liver over a large range of deformation consistent with the range of deformation in surgery. Based on the experimental data collected with the device during soft-tissue probing, we developed an axisymmetric finite-element model to characterize the material property *in vivo* of liver tissue. We did not consider the effect of the probe's geometrical shape on the tissue's stress field. The tissue was compressed up to 40% of its nominal thickness. While, in our present *in vivo* swine experiments, we were able to put a metal plate under the liver, this is not practical for measuring the liver characteristics for human organ testing. We will develop alternative approaches to make these measurements in human liver when we plan to do such experiments.

The work presented in this research represents the experimental setup toward developing a reality-based model for tool-tissue interaction during probing. We plan to do several *in vivo* experiments for various probing speeds to evaluate the effect of probing speed on tissue LEEM. Quantifying the local deformation resistance of the soft-tissue to probing *in vivo* through constitutive relationships will help us to describe the observed tissue response behavior more realistically. This will eventually help the graphics and haptics community to develop reality-based surgical simulators for probing soft-tissue.

REFERENCES

- [1] D. d'Aulignac, R. Balaniuk, and C. Laugier, "A Haptic Interface for a Virtual Exam of the Human Thigh," *Proceedings of the IEEE International Conference on Robotics & Automation*, pp. 2452-2456, 2000.
- [2] J. T. Hing, A. D. Brooks, and J. P. Desai, "A Biplanar Fluoroscopic Approach for the Measurement, Modeling, and Simulation of Needle and Soft tissue Interaction," *Medical Image Analysis*, vol. 11, pp. 62-78, 2007.
- [3] A. E. Kerdok, "Soft Tissue Characterization: Mechanical Property Determination from Biopsies to Whole Organs," *Whitaker Foundation Biomedical Research Conference*, 2001.
- [4] K. B. Arbogast, K. L. Thibault, B. S. Pinheiro, K. I. Winey, and S. S. Margulies, "A High-Frequency shear device for testing soft biological tissues," *Journal of Biomechanics*, vol. 30, pp. 757-759, 1997.
- [5] H. R. Halperin, J. E. Tsitlik, M. Gelfand, J. Downs, and F. C. P. Yin, "Servo-Controlled Indenter for determining the transverse stiffness of ventricular muscle," *IEEE Transactions on Biomedical Engineering*, vol. 38, pp. 602-607, 1991.
- [6] M. P. Ottensmeyer, "In vivo measurement of solid organ viscoelastic properties," *Medicine Meets Virtual Reality*, vol. 2, pp. 328-333, 2002.
- [7] Y. C. Fung, *Biomechanics: Mechanical properties of living tissues*, Second edition ed. New York: Springer-Verlag, 1993.
- [8] P. Tong and Y. C. Fung, "The Stress-Strain Relationship for the Skin," *J. Biomechanics*, vol. 9, pp. 649-657, 1976.
- [9] T. Hu and J. P. Desai, "A biomechanical model of the liver for reality-based haptic feedback," in *Medical Image Computing and Computer Assisted Intervention (MICCAI)*, Montreal, Canada, 2003.
- [10] M. F. Beatty, "Topics in finite elasticity: Hyperelasticity of rubber, elastomers, and biological tissues with examples," *Appl Mech Rev.*, vol. 40, p. 12, 1987.
- [11] M. Farshad, M. Barbezat, P. Flueler, F. Schmidlin, P. Graber, and P. Niederer, "Material Characterization of the Pig Kidney in Relation with the Biomechanical Analysis of Renal Trauma," *J. Biomechanics*, vol. 32, pp. 417-425, 1999.
- [12] P. J. Davies, F. J. Carter, and A. Cuschieri, "Mathematical Modeling for Keyhole Surgery Simulations: A Biomechanical Model for Spleen Tissue," *IMA J. Applied Math*, vol. 67, pp. 41-67, 2002.
- [13] K. Miller, "Constitutive model of brain tissue suitable for finite element analysis of surgical procedures," *Journal of Biomechanics*, vol. 32, pp. 531-597, 1999.
- [14] J. W. Melvin, R. L. Stalnaker, and V. L. Roberts, "Impact injury mechanisms in abdominal organs," *SAE Transactions*, pp. 115-126, 1973.
- [15] A. Nava, E. Mazza, F. Kleinermann, N. J. Avis, J. McClure, and M. Bajka, "Evaluation of the mechanical properties of human liver and kidney through aspiration experiments," *Technology and Health Care*, vol. 12, pp. 269-280, 2004.

- [16] F. J. Carter, A. Cuschieri, D. Mclean, P. J. Davies, and T. G. Frank, "Measurements and modelling of the compliance of human and porcine organs," *Medical Image Analysis*, vol. 5, pp. 231-236, 2001.
- [17] T. Hu and J. P. Desai, "Soft-tissue material properties under large deformation: Strain rate effect," in *26th Annual International Conference: IEEE Engineering in Medicine and Biology Society*, San Francisco, CA, 2004.
- [18] T. Hu and J. P. Desai, "Modeling Large Deformation in Soft-tissues: Experimental results and Analysis," in *Eurohaptics*, Germany, 2004.
- [19] T. Hu, "Reality-based Soft Tissue Probing: Experiments and Computational Model for Application to Minimally Invasive Surgery ", Ph.D. Thesis, Drexel University, Philadelphia, PA.
- [1] D. d'Aulignac, R. Balaniuk, and C. Laugier, "A Haptic Interface for a Virtual Exam of the Human Thigh," *Proceedings of the IEEE International Conference on Robotics & Automation*, pp. 2452-2456, 2000.
- [2] J. T. Hing, A. D. Brooks, and J. P. Desai, "A Biplanar Fluoroscopic Approach for the Measurement, Modeling, and Simulation of Needle and Soft tissue Interaction," *Medical Image Analysis*, vol. 11, pp. 62-78, 2007.
- [3] A. E. Kerdok, "Soft Tissue Characterization: Mechanical Property Determination from Biopsies to Whole Organs," *Whitaker Foundation Biomedical Research Conference*, 2001.
- [4] K. B. Arbogast, K. L. Thibault, B. S. Pinheiro, K. I. Winey, and S. S. Margulies, "A High-Frequency shear device for testing soft biological tissues," *Journal of Biomechanics*, vol. 30, pp. 757-759, 1997.
- [5] H. R. Halperin, J. E. Tsitlik, M. Gelfand, J. Downs, and F. C. P. Yin, "Servo-Controlled Indenter for determining the transverse stiffness of ventricular muscle," *IEEE Transactions on Biomedical Engineering*, vol. 38, pp. 602-607, 1991.
- [6] M. P. Ottensmeyer, "In vivo measurement of solid organ viscoelastic properties," *Medicine Meets Virtual Reality*, vol. 2, pp. 328-333, 2002.
- [7] Y. C. Fung, *Biomechanics: Mechanical properties of living tissues*, Second edition ed. New York: Springer-Verlag, 1993.
- [8] P. Tong and Y. C. Fung, "The Stress-Strain Relationship for the Skin," *J. Biomechanics*, vol. 9, pp. 649-657, 1976.
- [9] T. Hu and J. P. Desai, "A biomechanical model of the liver for reality-based haptic feedback," in *Medical Image Computing and Computer Assisted Intervention (MICCAI)*, Montreal, Canada, 2003.
- [10] M. F. Beatty, "Topics in finite elasticity: Hyperelasticity of rubber, elastomers, and biological tissues with examples," *Appl Mech Rev*, vol. 40, p. 12, 1987.
- [11] M. Farshad, M. Barbezat, P. Flueler, F. Schmidlin, P. Graber, and P. Niederer, "Material Characterization of the Pig Kidney in Relation with the Biomechanical Analysis of Renal Trauma," *J. Biomechanics*, vol. 32, pp. 417-425, 1999.
- [12] P. J. Davies, F. J. Carter, and A. Cuschieri, "Mathematical Modeling for Keyhole Surgery Simulations: A Biomechanical Model for Spleen Tissue," *IMA J. Applied Math*, vol. 67, pp. 41-67, 2002.
- [13] K. Miller, "Constitutive model of brain tissue suitable for finite element analysis of surgical procedures," *Journal of Biomechanics*, vol. 32, pp. 531-597, 1999.
- [14] J. W. Melvin, R. L. Stalnaker, and V. L. Roberts, "Impact injury mechanisms in abdominal organs," *SAE Transactions*, pp. 115-126, 1973.
- [15] A. Nava, E. Mazza, F. Kleineremann, N. J. Avis, J. McClure, and M. Bajka, "Evaluation of the mechanical properties of human liver and kidney through aspiration experiments," *Technology and Health Care*, vol. 12, pp. 269-280, 2004.
- [16] F. J. Carter, A. Cuschieri, D. Mclean, P. J. Davies, and T. G. Frank, "Measurements and modelling of the compliance of human and porcine organs," *Medical Image Analysis*, vol. 5, pp. 231-236, 2001.

- [17] T. Hu and J. P. Desai, "Soft-tissue material properties under large deformation: Strain rate effect," in *26th Annual International Conference: IEEE Engineering in Medicine and Biology Society*, San Francisco, CA, 2004.
- [18] T. Hu and J. P. Desai, "Modeling Large Deformation in Soft-tissues: Experimental results and Analysis," in *Eurohaptics*, Germany, 2004.
- [19] T. Hu, J. P. Desai, A. E. Castellanos, and A. C. W., Lau, "Modeling In vivo Soft Tissue Probing", The First IEEE/RAS-EMBS International Conference on Biomedical Robotics and Biomechanics, 2006, BioRob 2006, February 20-22, 2006 Page(s):537 – 542.
- [20] T. Hu, J. P. Desai, and A. C. W., Lau, "Direct and inverse problem models for large soft-tissue deformation: Application to haptic feedback in surgical simulation", Proceedings of 12th International Conference on Advanced Robotics, 2005, ICAR '05, 18-20 July 2005 Page(s):445 – 451.
- [21] T. Hu, " Reality-based Soft Tissue Probing: Experiments and Computational Model for Application to Minimally Invasive Surgery ", Ph.D. Thesis, Drexel University, Philadelphia, PA.

List of figure captions

Figure 1. Experimental setup for *ex vivo* testing.

Figure 2. Schematic of the *in vivo* soft-tissue testing device.

Figure 3. Prototype of the portable probe for *in vivo* tests.

Figure 4. LCD display for user interface.

Figure 5. Diagram of motion control, data acquisition, and data storage.

Figure 6. Calibration curve: Output voltage from load cell vs. measured force.

Figure 7. Velocity profile: Displacement of the probe versus time.

Figure 8. *In vivo* experimental setup.

Figure 9. *In vivo* probe attached to a surgical tractor and the overall probe fixturing assembly.

Figure 10. Experimental data from *ex vivo* probing of soft tissue.

Figure 11. Plot of force versus displacement data from *in vivo* tests.

Figure 12. LEEM value computed for the liver from *in vivo* experiments.